







Neutral ceramidase deficiency protects against cisplatin-induced acute kidney injury

Sophia M. Sears^{1,*} , Tess V. Dupre^{1,*}, Parag P. Shah^{2,3}, Deanna L. Davis¹, Mark A. Doll¹, Cierra N. Sharp¹, Alexis A. Vega⁴ , Judit Megyesi⁵, Levi J. Beverly^{1,2,3}, Ashley J. Snider⁶, Lina M. Obeid^{7,8,9}, Yusuf A. Hannun^{7,8,9}, and Leah J. Siskind^{1,3,*} 

From the ¹Department of Pharmacology & Toxicology, ²Department of Medicine, ³James Graham Brown Cancer Center, and ⁴Department of Biochemistry & Molecular Genetics, University of Louisville, Louisville, KY, USA; ⁵Division of Nephrology, Department of Internal Medicine, University of Arkansas for Medical Sciences and Central Arkansas Veterans Healthcare System, Little Rock, AR, USA; ⁶Department of Nutritional Sciences, College of Agriculture and Life Sciences, University of Arizona, Tucson, AZ, USA; ⁷Department of Medicine, ⁸Stony Brook Cancer Center, Stony Brook University, Stony Brook, NY, USA; ⁹Northport Veteran Affairs Medical Center, Northport, NY, USA

Abstract Cisplatin is a commonly used chemotherapeutic for the treatment of many solid organ cancers; however, its effectiveness is limited by the development of acute kidney injury (AKI) in 30% of patients. AKI is driven by proximal tubule cell death, leading to rapid decline in renal function. It has previously been shown that sphingolipid metabolism plays a role in regulating many of the biological processes involved in cisplatin-induced AKI. For example, neutral ceramidase (nCDase) is an enzyme responsible for converting ceramide into sphingosine, which is then phosphorylated to become sphingosine-1-phosphate, and our lab previously demonstrated that nCDase knockout (nCDase^{-/-}) in mouse embryonic fibroblasts led to resistance to nutrient and energy deprivation-induced cell death via upregulation of autophagic flux.  In this study, we further characterized the role of nCDase in AKI by demonstrating that nCDase^{-/-} mice are resistant to cisplatin-induced AKI. nCDase^{-/-} mice display improved kidney function, reduced injury and structural damage, lower rates of apoptosis, and less ER stress compared to wild-type mice following cisplatin treatment. Although the mechanism of protection is still unknown, we propose that it could be mediated by increased autophagy, as chloroquine treatment resensitized nCDase^{-/-} mice to AKI development. Taken together, we conclude that nCDase may represent a novel target to prevent cisplatin-induced nephrotoxicity.

Supplementary key words autophagy • ceramide • sphingosine-1-phosphate • renal disease • animal models • cisplatin • sphingosine metabolism • chemotherapy • ER stress • chloroquine

Cisplatin (*cis*-diamminedichloridoplatinum(II)) is an effective chemotherapeutic for the treatment of many solid organ cancers (1–3). Unfortunately, the success of

cisplatin in treating these cancers is limited by its nephrotoxicity. Thirty percent of patients treated with cisplatin develop cisplatin-induced acute kidney injury (AKI) (4–7). AKI is defined as a rapid decline in glomerular filtration rate, clinically measured by increases in blood urea nitrogen (BUN) or serum creatinine (SCr) (8). AKI is primarily mediated by renal proximal tubule cell death, inflammation, and impaired microvasculature (9). Development of AKI not only limits the ability to treat cancer patients but also puts patients at risk for long-term renal effects (8, 10, 11). As development of cisplatin-induced AKI is thought to be largely driven by cell death (4, 6), protecting proximal tubule cells from death is an attractive strategy to prevent kidney structural damage and maintain function. Sphingolipid metabolism in the kidney is recognized as a regulator of several cellular processes, including cell death, that play a role in the development of AKI and other renal diseases (12–14); thus, this connection has been explored by our lab.

Sphingolipids are a class of bioactive lipids with a common sphingoid base backbone. Sphingolipid metabolism centers around the formation and breakdown of ceramides (15, 16). Neutral ceramidase (nCDase) is an enzyme involved in sphingolipid metabolism that cleaves ceramide into sphingosine, which is then recycled back to ceramide or phosphorylated to become sphingosine-1-phosphate (SIP) (17–20). The balance of these three bioactive lipids is regulated by dynamic processes and is thought to play an important role in regulating cellular stress responses (15, 16). In particular, ceramide, sphingosine, and SIP have been implicated in regulation of cell death and autophagy (16). Manipulating the balance of ceramide has also been shown to play a role in cisplatin-induced AKI. Inhibition of ceramide generation protected mice from cisplatin-induced AKI, while inhibition of glucosylceramide

*These authors contributed equally to this work.

*For correspondence: Leah J. Siskind, leah.siskind@louisville.edu.

synthase, an enzyme that glycosylates ceramide species to generate glycosphingolipids, exacerbated cisplatin-induced AKI (21).

Our lab demonstrated that nCDase knockout (nCDase^{-/-}) in mouse embryonic fibroblasts protected cells from nutrient and energy deprivation-induced cell death (22). This protection was mediated via upregulation of autophagy and mitophagy (22). Autophagy is known to play a protective role in cisplatin-induced AKI by decreasing levels of apoptotic cell death (23, 24). Additionally, nCDase^{-/-} mice were found to be protected in a model of traumatic brain injury due to preservation of mitochondrial function (25). Mitochondrial dysfunction is also known to be a major mediator of cisplatin-induced AKI (4). Therefore, we hypothesized that nCDase deficiency would prevent development of cisplatin-induced AKI via upregulation of autophagy and inhibition of cell death.

In this study, we utilized wild-type and nCDase^{-/-} C57BL/6 mice in the cisplatin-induced AKI model. Our data demonstrate that loss of nCDase attenuates AKI development following 20 mg/kg cisplatin treatment as evidenced by markers of kidney function, kidney injury, cell death, and kidney pathology. Furthermore, we demonstrate that chloroquine (CQ) treatment exacerbates development of AKI in nCDase^{-/-} mice. This suggests that nCDase deficiency could be mediating protection from cisplatin-induced AKI by increasing basal autophagy and allowing cells to survive cisplatin-induced injury. These data indicate that nCDase may be a feasible target for prevention of cisplatin nephrotoxicity.

MATERIALS AND METHODS

Animals

nCDase^{-/-} mice were generated in the laboratory of Dr Richard L. Proia (NIDDK, National Institutes of Health) (26). These mice were backcrossed for 10 generations onto a C57BL/6 background (27). nCDase^{-/-} knockout mice were bred in-house, and all experiments were performed at 8 weeks of age. Wild-type mice (C57BL/6, male, 8 weeks old) were either bred in-house or purchased from The Jackson Laboratory (Bar Harbor, ME) and allowed to acclimate for 4 weeks prior to initiation of experiments. All mice were maintained on a 12-h light–dark cycle and provided food and water ad libitum. All animal procedures were approved by the Institutional Animal Care and Use Committee and followed the guidelines of the American Veterinary Medical Association. Pharmacy grade cisplatin (1 mg/ml) from either Teva or Intas Pharmaceuticals was obtained from the University of Louisville Hospital pharmacy. Cisplatin 20 mg/kg (in 0.9% normal saline) was administered by intraperitoneal injection at time zero. All animals were injected with cisplatin at the same time of the day as there are circadian influences on the response of the kidney to cisplatin (28, 29). CQ diphosphate salt (Sigma-Aldrich, C6628) was dissolved in 0.9% normal saline into a 15 mg/ml stock solution. Mice were intraperitoneally injected with CQ at 60 mg/kg in 0.9% normal saline 1 h before cisplatin dosing and 24 and 48 h after dosing. Euthanasia was performed 72 h after cisplatin dosing. Blood was

collected and plasma was prepared and frozen at -80°C; urine and kidneys were collected, flash frozen in liquid nitrogen, and stored at -80°C until use; one kidney was sliced and fixed in 10% neutral-buffered formalin.

Assessment of kidney function and injury markers

BUN (AMS Diagnostics, 40146) and SCr (Point Scientific Inc, C7548-120) levels were determined on plasma samples using kits, following the manufacturers' instructions. ELISAs for neutrophil gelatinase-associated lipocalin (NGAL) (R&D Systems, DY1857) were performed on the urine as directed by the manufacturer and as previously described (30).

Protein quantification and Western blot analysis

Homogenates were made from kidney cortex using cell extraction buffer (Thermo Fisher Scientific, FNN0011), containing a cOMplete protease inhibitor cocktail tablet (Roche, 4693159001) and PhosSTOP phosphatase inhibitor cocktail tablet (Roche, 4906837001). Protein concentrations were determined using Bradford Reagent (Bio-Rad, 5000001). Kidney homogenate (40 µg) was separated on 4%–12% gradient Tris–Glycine–SDS polyacrylamide gels, transferred to PVDF membranes, and proteins were detected by chemiluminescence substrate. Antibodies were purchased from Cell Signaling unless otherwise noted: inositol requiring enzyme-1α, #3294; extracellular receptor kinase (ERK), #4695; phosphorylated-ERK(p-ERK), #4370; cleaved caspase 3 (CC3), #9664; C/EBP homologous protein, #2895; c-jun n-terminal kinase (JNK), #9258; phosphorylated-JNK (p-JNK), #4668; proliferating cell nuclear antigen (PCNA), #13110; phosphorylated-eukaryotic initiation factor 2α, #3398; sequestosome 1/p62 (p62), #5114; microtubule-associated protein light chain 3, #3868; α-tubulin (Santa Cruz Biotechnology, sc-5286) and β-actin (Sigma-Aldrich, A2228).

Gene expression

RNA was isolated using TRIzol (Thermo Fisher Scientific, 15596026) or EZ.N.A. Total RNA Kit (Omega, R6834-02) per the manufacturers' protocol. Complementary DNA was synthesized from 1 µg RNA with High-Capacity cDNA Reverse Transcriptase PCR (Life Technologies, 4368814) per the manufacturer's instructions. The following TAQ-man assays (Life Technologies) were used: tumor necrosis factor α (*Tnfa*, Mm00443258_m1), interleukin-6 (*Il-6*, Mm00446190_m1), chemokine (C-X-C Motif) ligand 1 (*Cxcl1*, Mm04207460_m1), monocyte chemoattractant protein-1 (*Mcp-1*, Mm00-441242_m1), and the housekeeping gene beta-2-microglobulin (*B2m*, Mm00437762_m1). The primer for kidney injury molecule-1 was self-designed with the following sequences: forward AGATCCACACATGTACCAACATCAA and reverse CAGTGCCATTCCAGTCTGGTTT. Real-time quantitative RT-PCR was done with either iTaq Universal Probes Supermix (Bio-Rad, 172-5134) or iTaq Universal Sybr Green Supermix (Bio-Rad, 172-5124).

Histology

Kidney histology and immunohistochemistry were done as previously described (30–32). Briefly, kidney sections (5 µm) were stained with H&E and periodic acid–Schiff (PAS), and the degree of morphologic changes was determined by light microscopy in a blinded fashion. The following measures were chosen as an indication of morphologic damage to the kidney after drug treatment: proximal tubule degeneration,

loss of brush border, tubular casts, proximal tubule dilation, and proximal tubule necrosis. These measures were evaluated on a scale from 0 to 4, which ranged from not present (0), mild (1), moderate (2), severe (3), and very severe (4).

TUNEL staining

ApopTag Red In Situ Apoptosis Detection Kit (Millipore, S7165) was used for immunofluorescent detection of apoptotic cells following the manufacturer's protocol. ApopTag Plus Peroxidase In Situ Apoptosis Kit (Millipore, S7101) was used for bright-field detection of apoptotic cells following the manufacturer's protocol.

Statistical analysis

Data are expressed as means \pm SEM for all experiments. Multiple comparisons of normally distributed data were analyzed by two-way ANOVA, as appropriate, and group means were compared using Tukey post-tests. The criterion for statistical differences was $P < 0.05$ for all comparisons.

RESULTS

nCDase^{-/-} mice are resistant to cisplatin-induced AKI

Seventy-two hours post treatment with 20 mg/kg cisplatin, nCDase^{-/-} mice demonstrated improved renal function with significantly reduced BUN (Fig. 1A) and lower levels of SCr (Fig. 1B) than wild-type cisplatin-treated mice. Kidney injury, measured by

urinary NGAL, was also decreased in nCDase^{-/-} mice (Fig. 1C). Overt toxicity, as indicated by greater than 10% body weight loss, was comparable between wild-type and nCDase^{-/-} mice (Fig. 1D).

Cisplatin-induced AKI presents with tubular necrosis, loss of brush border, regeneration, cast formation, degeneration, and dilation (33). H&E-stained and PAS-stained kidney sections of nCDase^{-/-} and wild-type mice were scored by a pathologist in a blinded manner. Histology demonstrated improvement in tissue damage in nCDase^{-/-} mice, with significantly less tubular necrosis, loss of brush border, and tubular cast formation compared with wild-type cisplatin-treated mice (Fig. 2A–D). There was also less tubule degeneration and dilation in nCDase^{-/-} mice, although results were not significant (Fig. 2F, G).

nCDase^{-/-} mice had significantly less inflammatory cells present in the kidney as measured by pathology compared to wild-type mice 72 h post cisplatin treatment (Fig. 2E). This corresponds with lower mRNA expression of inflammatory cytokines *Tnfa*, *Il-6*, *Mcp-1*, and *Cxcl1* in the kidney cortex of cisplatin-treated nCDase^{-/-} mice compared to wild-type cisplatin-treated mice (Fig. 3A–D). Taken together, these results indicate that nCDase^{-/-} mice had improved kidney function, less injury, less structural damage, and less inflammation as compared to wild-type mice 72 h post cisplatin treatment.

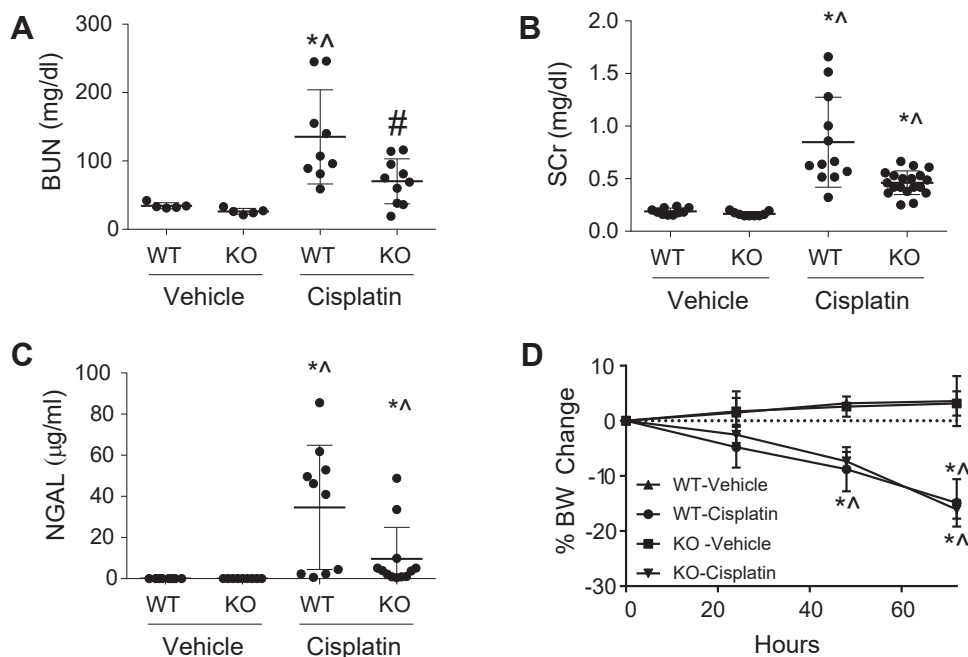


Fig. 1. Loss of neutral ceramidase (nCDase) attenuates cisplatin-induced acute kidney injury (AKI). Markers of kidney function: (A) blood urea nitrogen (BUN) and (B) serum creatinine (SCr) were measured from plasma 72 h following administration of cisplatin (20 mg/kg, ip.) or vehicle. C: Urinary neutrophil gelatinase-associated lipocalin (NGAL) was assessed 72 h following cisplatin administration. D: Percent body weight (BW) change from baseline was monitored each day after injection. WT indicates wild-type mice and KO indicates nCDase^{-/-} mice. Statistical differences were determined by a two-way ANOVA followed by a Tukey post-test. *Statistically different than vehicle-treated WT mice. #Statistically different than cisplatin-treated WT mice. †Statistically different than vehicle-treated KO mice. Data expressed as mean \pm SEM, $n = 5-10$.

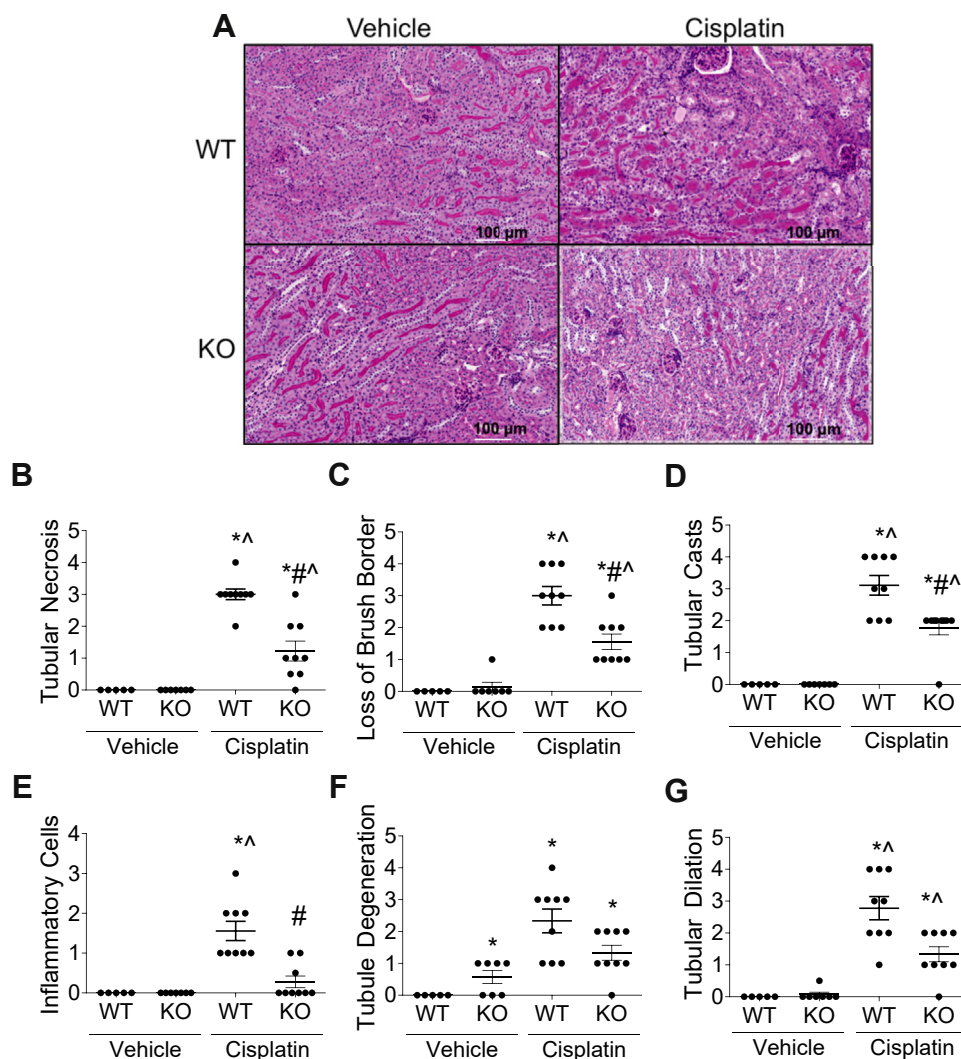


Fig. 2. Loss of neutral ceramidase (nCDase) protects from cisplatin-induced deterioration in kidney pathology. Mice were euthanized 72 h following 20 mg/kg intraperitoneal cisplatin or vehicle treatment. Renal histological changes were assessed on 5- μ m-thick paraffin-embedded, H&E and PAS-stained sections. A: Representative images of renal histology. B: Tubular necrosis, (C) loss of proximal tubule brush borders, (D) proximal tubule cast formation, (E) inflammatory cells, (F) tubule degeneration, and (G) tubule dilation were assessed as markers of histological changes. For figures (B–G), scoring of the sections was performed in a blinded manner by renal pathologist Dr Megyesi using a scale of 0–4 (0 = not present, 1 = mild, 2 = moderate, 3 = severe, and 4 = very severe renal histological changes in the proximal tubules). WT indicates wild-type mice and KO indicates nCDase^{-/-} mice. Statistical differences were measured by individual chi-square tests. *Statistically different than vehicle-treated WT mice. #Statistically different than cisplatin-treated WT mice. ^Statistically different than vehicle-treated KO mice. Data expressed as mean \pm SEM, n = 5–10.

nCDase^{-/-} mice have lower levels of apoptosis and ER stress induction following 20 mg/kg cisplatin treatment

A hallmark of cisplatin-induced AKI is induction of cell death. nCDase^{-/-} mice treated with cisplatin had no detectable expression of CC3, a marker of apoptosis, whereas cisplatin-treated wild-type mice had obvious induction of CC3 expression (Fig. 4A). TUNEL staining was also performed to assess DNA breaks formed during apoptosis. nCDase^{-/-} mice had significantly less TUNEL+ cells compared to wild-type mice after cisplatin treatment (Fig. 4B, C). Lastly, PCNA expression was measured to assess the level of cell proliferation occurring in the kidney after cisplatin treatment.

nCDase^{-/-} mice had reduced PCNA induction by cisplatin compared to wild-type mice (Fig. 5). These results indicate that nCDase^{-/-} mice are protected from apoptotic cell death and cellular proliferation following 20 mg/kg cisplatin treatment.

Cisplatin is also known to induce ER stress, often leading to cell death (34). ER stress induction was assessed via protein expression of p-ERK, p-JNK, p-eIF2 α , and CHOP. Cisplatin-treated nCDase^{-/-} mice had lower expression of these markers compared to cisplatin-treated wild-type mice (Fig. 5). These results suggest that nCDase^{-/-} mice are resistant to ER stress induction in the kidney following 20 mg/kg cisplatin treatment.

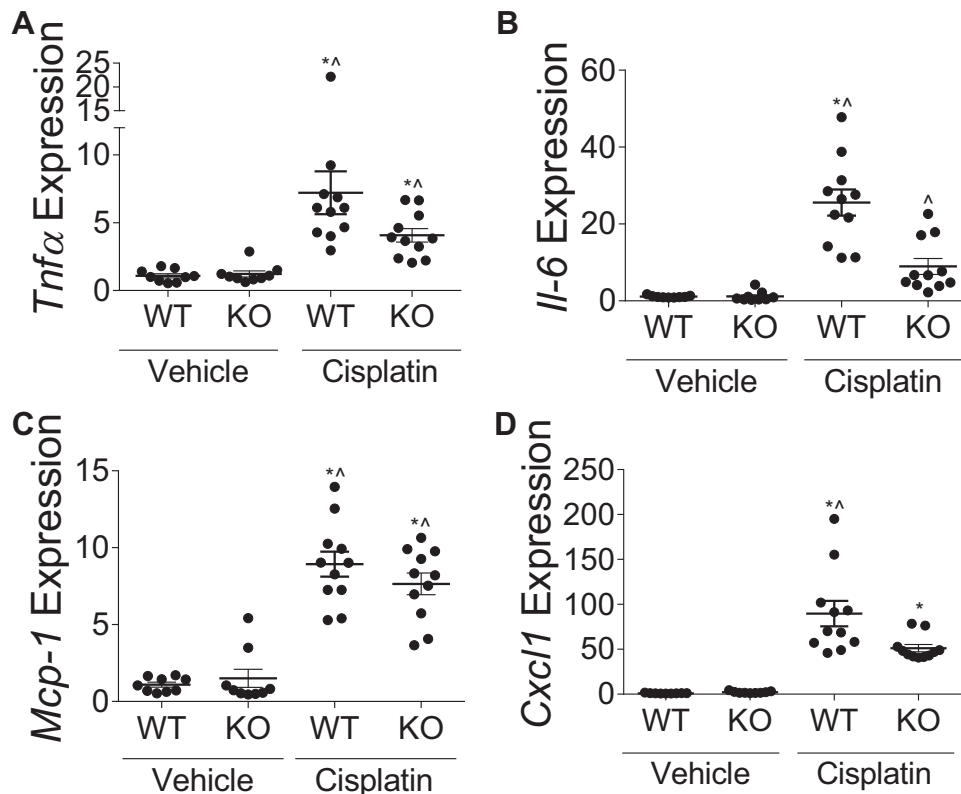


Fig. 3. Loss of neutral ceramidase (nCDase) decreases inflammatory cytokine and chemokine production in the kidney following cisplatin treatment. Mice were euthanized 72 h following 20 mg/kg intraperitoneal cisplatin or vehicle treatment. mRNA expression relative to control gene beta-2-microglobulin of (A) tumor necrosis factor- α (*Tnf α*), (B) interleukin-6 (*Il-6*), (C) monocyte chemoattractant protein-1 (*Mcp-1*), and (D) chemokine (C-X-C) ligand-1 (*Cxcl1*) were measured via real-time qRT-PCR. WT indicates wild-type mice and KO indicates nCDase^{-/-} mice. Statistical differences were determined by two-way ANOVA followed by Tukey post-test. *Statistically different than vehicle-treated WT mice. #Statistically different than cisplatin-treated WT mice. ^Statistically different than vehicle-treated KO mice. Data expressed as mean \pm SEM, n = 5–10.

CQ treatment inhibits autophagy in cisplatin-treated nCDase^{-/-} mice

We first examined basal expression of LC3 in the kidneys of nCDase^{-/-} and wild-type mice. nCDase^{-/-} mice increased expression of LC3 compared to wild-type mice, suggesting upregulation of autophagy (Fig. 6A). nCDase^{-/-} mice were then administered 60 mg/kg CQ 1 h before cisplatin treatment and 24 and 48 h after treatment. This dosing regimen of CQ was chosen as it was shown to inhibit autophagy in the kidney of C57BL/6 wild-type mice by other groups (23). We observed expression of autophagy markers LC3 and p62 in the kidney 72 h after cisplatin treatment. Interestingly, basal autophagy levels in the kidney of nCDase^{-/-} mice seemed unaltered by CQ treatment. However, CQ inhibited cisplatin-induced autophagy in the kidney at this time point as evidenced by increased LC3-II and p62 expression (Fig. 6B–D). Increased expression of these markers occurs as CQ prevents autophagic flux by blocking autophagosome fusion with the lysosome (35).

CQ treatment exacerbates cisplatin-induced AKI and apoptosis in nCDase^{-/-} mice

nCDase^{-/-} mice treated with CQ and cisplatin had increased BUN and NGAL levels compared to

nCDase^{-/-} mice treated with cisplatin alone (Fig. 7A, C). CQ treatment also led to a significant increase in mRNA expression of the AKI biomarker kidney injury molecule-1 in the kidney following cisplatin treatment (Fig. 7B). Body weight loss was less dramatic in cisplatin- and CQ-treated mice compared to cisplatin alone-treated mice, but both groups surpassed 10% body weight loss indicating overt toxicity (Fig. 7D).

Cisplatin-induced inflammatory cytokine production was also exacerbated by CQ treatment in the kidney cortex of nCDase^{-/-} mice. *Tnf α* , *Il-6*, *Mcp-1*, and *Cxcl1* mRNA expressions were all significantly elevated in the kidney of CQ and cisplatin-treated nCDase^{-/-} mice compared to cisplatin-treated nCDase^{-/-} mice (Fig. 8). These results indicate that CQ treatment in nCDase^{-/-} mice increases functional loss, kidney injury, and inflammatory cytokine production following cisplatin treatment.

Apoptosis was examined in nCDase^{-/-} mice treated with CQ and cisplatin via CC3 expression and TUNEL staining. CC3 expression was elevated in nCDase^{-/-} mice treated with CQ and cisplatin compared to nCDase^{-/-} mice treated with cisplatin alone (Fig. 9A). Similarly, CQ treatment increased the number of TUNEL+ cells in nCDase^{-/-} mice following cisplatin treatment (Fig. 9B, C). These results suggest that CQ

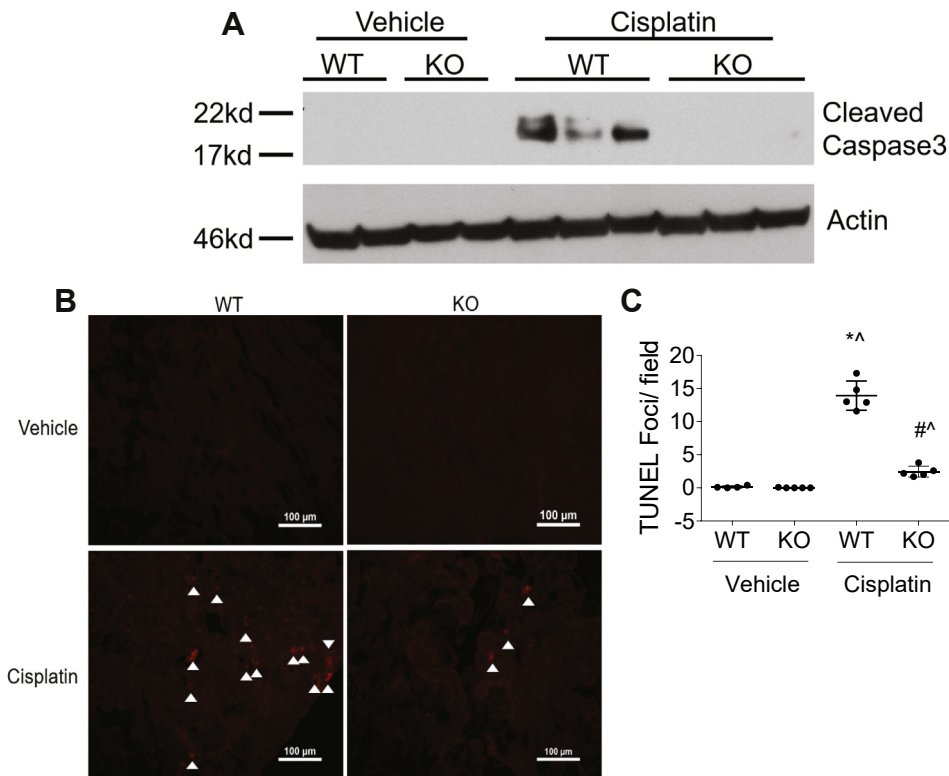


Fig. 4. Loss of neutral ceramidase (nCDase) attenuates cisplatin-induced apoptosis. **A:** Western blot analysis was performed to assess relative protein levels of the indicated proteins in the renal cortex of mice. Samples from the kidney cortex were prepared from mice euthanized 72 h after cisplatin administration. $n = 2-3$. The same protein lysates and loading control gene were used for **Figures 5** and **6A**. **B, C:** TUNEL assays were performed on paraffin-embedded kidney sections as an index of apoptosis. **B:** Representative photomicrographs of TUNEL assays. **C:** TUNEL quantification. Statistical differences were measured by two-way ANOVA followed by Tukey post-test. Data expressed as mean \pm SEM. $n = 5$. WT indicates wild-type mice and KO indicates nCDase^{-/-} mice. *Statistically different than vehicle-treated WT. #Statistically different than cisplatin-treated WT. ^Statistically different from vehicle-treated KO.

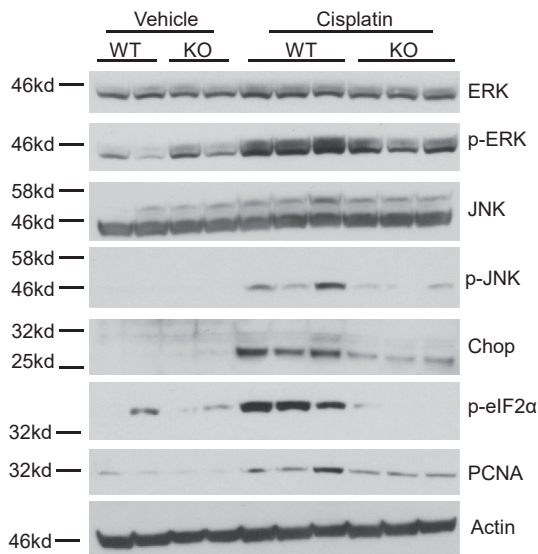


Fig. 5. Loss of neutral ceramidase (nCDase) attenuates cisplatin-induced ER stress and proliferation. Western blot analysis was performed to assess relative protein levels of the indicated proteins in the renal cortex of mice. Samples from the kidney cortex were prepared from mice sacrificed 72 h after cisplatin administration. WT indicates wild-type mice and KO indicates nCDase^{-/-} mice. $n = 2-3$. The same protein lysates and loading control gene were used for **Figures 4A** and **6A**.

treatment exacerbates cisplatin-induced apoptosis in nCDase^{-/-} mice. Wild-type C57BL/6 mice were not used in this experiment as it was previously published that CQ treatment exacerbated cisplatin-induced AKI in these mice (23).

DISCUSSION

Sphingolipid metabolism is increasingly recognized as an important player in the development of kidney injury and disease (14). Our lab has demonstrated that manipulation of the generation and breakdown of ceramides can alter sensitivity to cisplatin-induced AKI (21). Additionally, we have shown that nCDase knockout protects mouse embryonic fibroblasts from nutrient and energy deprivation-induced cell death via upregulation of autophagic flux (22). Autophagy has also been shown to be protective from cisplatin-induced AKI (23). Therefore, we hypothesized that nCDase^{-/-} mice would be protected from cisplatin-induced AKI.

In this study, we demonstrate that nCDase^{-/-} mice have improved renal function, less kidney injury, and less tubule structural damage following 20 mg/kg cisplatin treatment compared to wild-type mice.

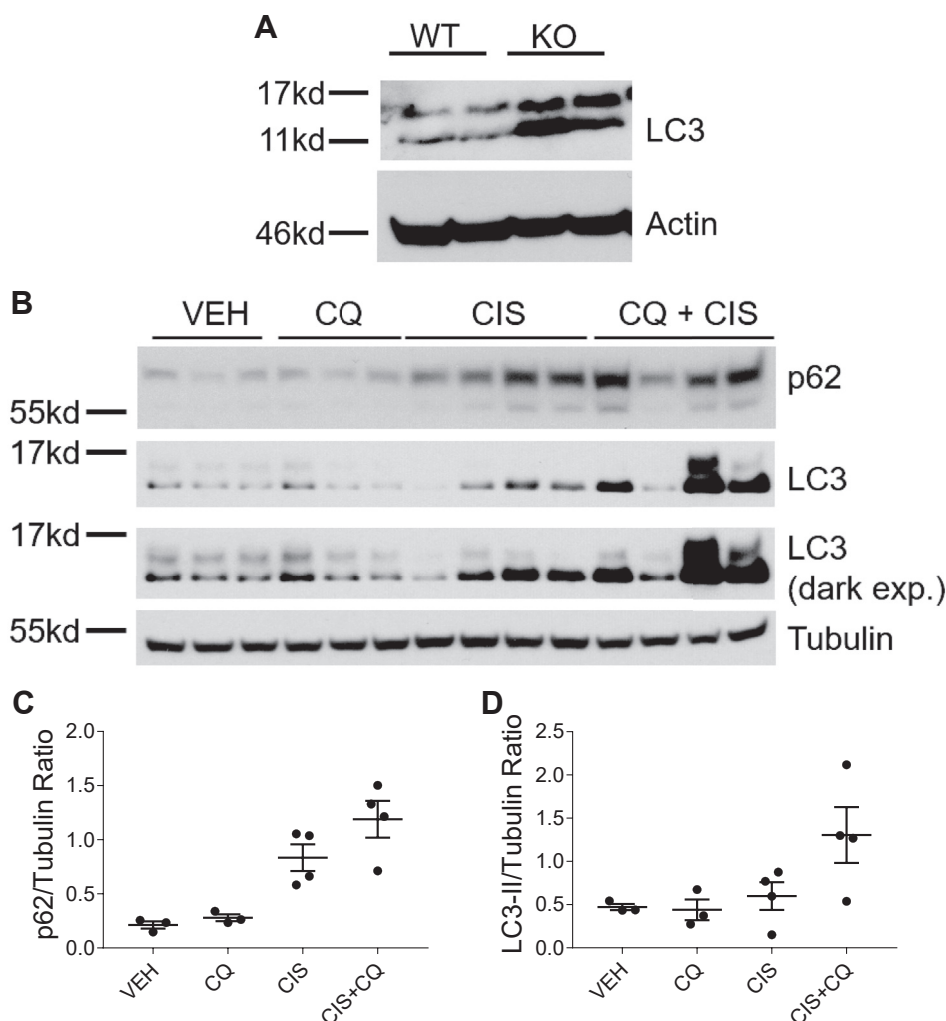


Fig. 6. Chloroquine inhibits autophagy induction in cisplatin-treated neutral ceramidase knockout ($nCDase^{-/-}$) mice. **A:** Western blot analysis was performed to assess relative basal protein levels of the indicated proteins in the renal cortex of $nCDase^{-/-}$ and wild-type mice. $n = 2$. The same protein lysates and loading control gene were used for Figures 4A and 5. **B:** Mice were euthanized 72 h following treatment. Western blot analysis was performed to assess relative protein levels of the indicated proteins in the renal cortex of $nCDase^{-/-}$ mice. $n = 3-4$. VEH indicates vehicle-treated $nCDase^{-/-}$ mice, CQ indicates chloroquine-treated $nCDase^{-/-}$ mice, CIS indicates cisplatin-treated $nCDase^{-/-}$ mice, and CIS+CQ indicates cisplatin and chloroquine-treated $nCDase^{-/-}$ mice. The same protein lysates and loading control gene were used for Figure 9A. **C:** Quantification of p62 expression relative to tubulin. **D:** Quantification of LC3II expression relative to tubulin.

Additionally, $nCDase^{-/-}$ mice are protected from cisplatin-induced apoptosis and ER stress induction. We believe this protection is mediated by basally increased levels of autophagy in the kidney. LC3 expression was elevated in the kidneys of $nCDase^{-/-}$ mice compared to wild-type mice. $nCDase^{-/-}$ knockout in mouse embryonic fibroblasts was also previously shown to increase autophagic flux (22). Furthermore, CQ treatment sensitized $nCDase^{-/-}$ mice to cisplatin-induced AKI. $nCDase^{-/-}$ mice treated with CQ and cisplatin had worsened renal function, higher levels of kidney injury, and more apoptosis compared to $nCDase^{-/-}$ mice treated with cisplatin alone.

We believe this sensitization is due to autophagy inhibition; however, it is important to note that CQ is known to affect cellular processes other than autophagy. CQ is a weak base and will therefore accumulate

in any acidic cellular compartment. Lysosome morphology, Golgi organization, and endosomal trafficking were altered in several cell lines by CQ treatment (35). Additionally, CQ has been shown to affect membrane stability, signaling pathways, and immune activation (36, 37). We cannot definitively conclude that CQ is resensitizing $nCDase^{-/-}$ mice to cisplatin-induced AKI via autophagy inhibition. Therefore, we also cannot conclude that $nCDase^{-/-}$ knockout mediates protection from cisplatin-induced AKI via upregulation of autophagy. However, based on our previous in vitro work (22), we believe this is the primary mechanism of action, and increased autophagy is reducing cell death in the kidney following cisplatin treatment.

Ceramide generation has also been implicated in the regulation of cell death (15). Different forms of cellular

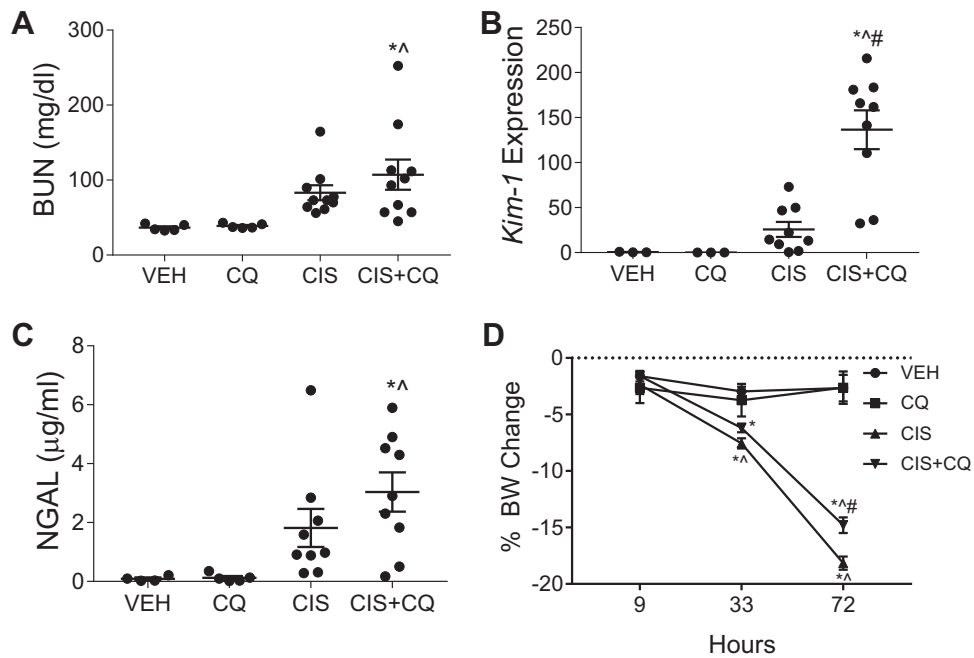


Fig. 7. Chloroquine exacerbates cisplatin-induced AKI in neutral ceramidase knockout (nCDase^{-/-}) mice. Mice were sacrificed 72 h following treatment. A: Blood urea nitrogen (BUN) was measured from plasma. B: Kidney injury molecule 1 (Kim-1) mRNA was measured by qRT-PCR from the renal cortex. C: Urinary NGAL was assessed. D: Percent body weight (BW) change from baseline was monitored each day after injection. VEH indicates vehicle-treated nCDase^{-/-} mice, CQ indicates chloroquine-treated nCDase^{-/-} mice, CIS indicates cisplatin-treated nCDase^{-/-} mice, and CIS+CQ indicates cisplatin and chloroquine-treated nCDase^{-/-} mice. Statistical differences were determined by a two-way ANOVA followed by a Tukey post-test. *Statistically different than vehicle-treated mice. #Statistically different than cisplatin-treated mice. ^Statistically different than chloroquine-treated mice. Data expressed as mean ± SEM, n = 5–10.

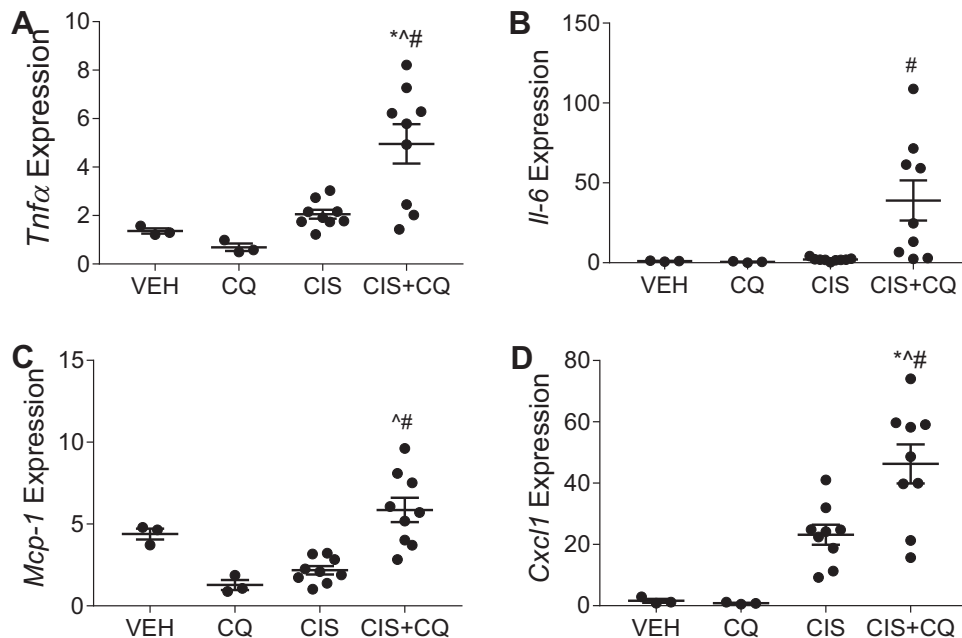


Fig. 8. Chloroquine exacerbates inflammatory cytokine and chemokine production in neutral ceramidase knockout (nCDase^{-/-}) mice. Mice were sacrificed 72 h following treatment. mRNA expression relative to control gene beta-2-microglobulin of (A) tumor necrosis factor α (*Tnfα*), (B) interleukin-6 (*Il-6*), (C) monocyte chemoattractant protein-1 (*Mcp-1*), and (D) chemokine (C-X-C) ligand-1 (*Cxc1*) were measured via real-time qRT-PCR. VEH indicates vehicle-treated nCDase^{-/-} mice, CQ indicates chloroquine-treated nCDase^{-/-} mice, CIS indicates cisplatin-treated nCDase^{-/-} mice, and CIS+CQ indicates cisplatin and chloroquine-treated nCDase^{-/-} mice. Statistical differences were determined by a two-way ANOVA followed by a Tukey post-test. *Statistically different than vehicle-treated mice. #Statistically different than cisplatin-treated mice. ^Statistically different than chloroquine-treated mice. Data expressed as mean ± SEM, n = 5–10.

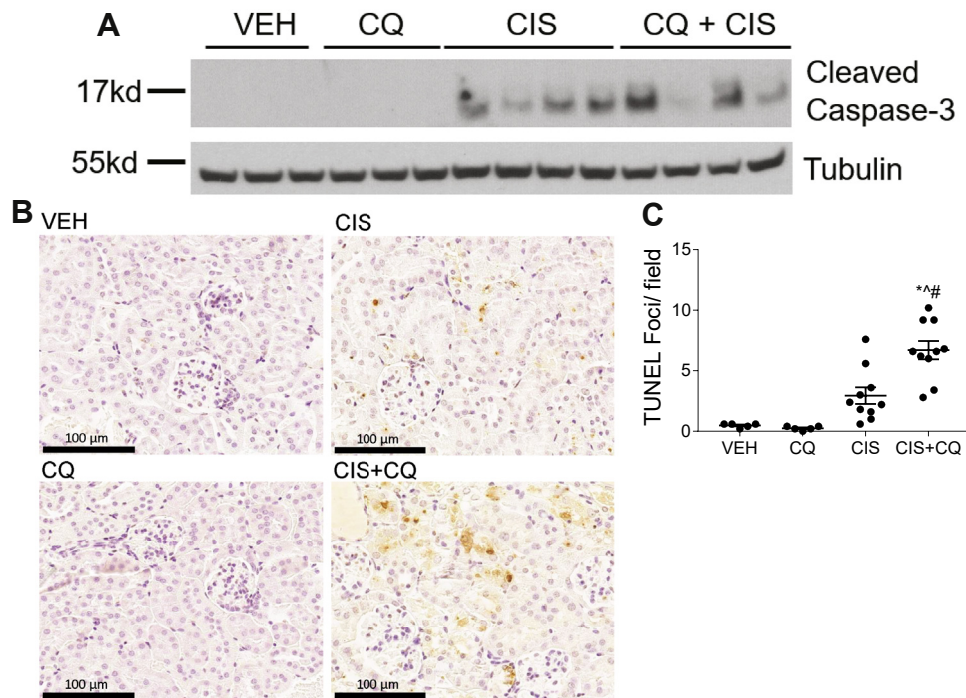


Fig. 9. Chloroquine exacerbates cisplatin-induced apoptosis in neutral ceramidase knockout ($nCDase^{-/-}$) mice. Mice were sacrificed 72 h following treatment. **A:** Western blot analysis was performed to assess relative protein levels of the indicated proteins in the renal cortex of mice. $n = 3-4$. The same protein lysates and loading control gene were used for Figure 6B. **B, C:** TUNEL assays were performed on paraffin-embedded kidney sections as an index of apoptosis. **B:** Representative images of TUNEL assays. **C:** TUNEL quantification. Statistical differences were measured by two-way ANOVA followed by Tukey post-test. Data expressed as mean \pm SEM. $n = 5-10$. VEH indicates vehicle-treated $nCDase^{-/-}$ mice, CQ indicated chloroquine-treated $nCDase^{-/-}$ mice, CIS indicates cisplatin-treated $nCDase^{-/-}$ mice, and CIS+CQ indicates cisplatin and chloroquine-treated $nCDase^{-/-}$ mice. Statistical differences were determined by a two-way ANOVA followed by a Tukey post-test. *Statistically different than vehicle-treated mice. #Statistically different than cisplatin-treated mice. Statistically different than chloroquine-treated mice. Data expressed as mean \pm SEM, $n = 5-10$.

stress, including cisplatin treatment, have been shown to induce ceramide accumulation and apoptosis in vitro (38, 39). Furthermore, inhibition of de novo ceramide synthesis prevented stress-induced apoptosis (38). As $nCDase$ is responsible for the breakdown of ceramide into sphingosine and SIP, it may seem counter intuitive that $nCDase$ inhibition would lead to decreased levels of cisplatin-induced apoptosis. However, inhibition of sphingolipid metabolizing enzymes does not always alter lipid levels in an expected way because of the complexity and interconnectedness of sphingolipid metabolic pathways. For example, loss of $nCDase$ could be causing alterations in glycosphingolipid levels which have been shown to play a role in cisplatin-induced AKI (21). Additionally, sphingosine has also been shown to promote proximal tubule cell injury in vitro (40), suggesting that $nCDase^{-/-}$ knockout could be protective by decreasing sphingosine levels in the kidney. Other studies have also demonstrated how $nCDase$ loss can cause unexpected changes in the balance of ceramide, sphingosine, and SIP.

Snider *et al.* (41) demonstrated that $nCDase^{-/-}$ mice had increased levels of SIP in colon epithelium compared to wild-type mice. These data suggest that $nCDase^{-/-}$ mice could be protected by a counterintuitive increase in SIP and SIP receptor 1 (SIPR1)


activation. SIPR1 activity has been shown to attenuate cisplatin-induced AKI by decreasing mitochondrial dysfunction and subsequent apoptosis (42). Additionally, the Okusa laboratory has shown a protective role for SIPR1 in both proximal tubule cells and endothelial cells in a model of renal ischemia/reperfusion-induced AKI (43-46). However, studies show that activation of SIPR3 in dendritic cells is detrimental to renal ischemia/reperfusion-induced AKI (47, 48). It should be noted that it is difficult to assess how loss of $nCDase$ is altering sphingosine and SIP levels in cisplatin-induced AKI as the effects may be cell type-specific and lipidomics analysis only allows us to assess steady state levels of whole tissue homogenates. Future studies employing in-depth lipidomics and MALDI imaging mass spectrometry (to get at the spatial changes in lipids) are needed to identify the lipid species involved. Additionally, future studies utilizing cell type-specific $nCDase^{-/-}$ mice are important to better understand how loss of $nCDase$ is attenuating cisplatin-induced AKI.

We hypothesize that $nCDase^{-/-}$ knockout mediates protection from cisplatin-induced apoptosis and ER stress via upregulation of autophagy. Although the balance of ceramide, sphingosine, and SIP has been shown to affect levels of autophagy, the relationship is

often determined by cell type and even subcellular localization of these lipids (49). Ceramide has been shown to induce autophagy (50, 51); however, SIP has also been shown to induce autophagy (52, 53). Interestingly, nCDase inhibition was also shown to increase autophagy in colon cancer cells (27). The molecular mechanisms by which nCDase regulates autophagic flux requires further investigation.

This study presents nCDase as a viable target for preventing cisplatin-induced AKI. We demonstrate that nCDase^{-/-} mice are protected from cisplatin-induced AKI as measured by decreased levels of apoptosis and ER stress. Interestingly, literature also supports nCDase inhibition as a strategy in treating colon cancer (27). Future studies should be aimed at identifying how nCDase inhibition may affect cancer treatment with cisplatin. It is also important to evaluate how nCDase inhibition alters long-term renal outcomes following cisplatin treatment, as cisplatin has been shown to induce renal fibrosis in mice given repeated low doses of cisplatin (30, 54). nCDase inhibition may play different roles in the biological processes occurring in chronic kidney injury (55). Taken together, these studies present nCDase inhibition as a novel target to prevent cisplatin nephrotoxicity and thereby improve cancer treatment.

Data availability

All data described are contained within this manuscript. 

Acknowledgments

The authors would like to thank the Sphingolipid Animal Cancer Pathobiology Shared Resource Core (P01CA097132) for the nCDase^{-/-} mice.

Author contributions

S. M. S., T. V. D., L. J. B., A. J. S., L. M. O., Y. A. H., and L. J. S. conceptualization; S. M. S., T. V. D., L. J. B., A. J. S., L. M. O., Y. A. H., and L. J. S. methodology; S. M. S., T. V. D., and D. L. D. investigation; S. M. S., T. V. D., P. P. S., D. L. D., M. A. D., C. N. S., A. A. V., and J. M. formal analysis; S. M. S. and T. V. D. data curation; S. M. S. and T. V. D. writing—original draft; S. M. S., T. V. D., P. P. S., D. L. D., M. A. D., C. N. S., A. A. V., J. M., L. J. B., A. J. S., L. M. O., Y. A. H., and L. J. S. writing—review and editing.

Author ORCIDiDs

Sophia M. Sears  <https://orcid.org/0000-0003-2396-5385>

Alexis A. Vega  <https://orcid.org/0000-0002-9359-6880>

Leah J. Siskind  <https://orcid.org/0000-0001-5026-5187>

Funding and additional information

This work was supported by the National Institutes of Health [R01DK124112 to L. J. S., F31DK126400 to S. M. S., PO1CA097132 to L. M. O. and Y. A. H.]; and VA Merit Awards [CAMM-011-13S to L. M. O.]. *The content is solely the responsibility of the authors and do not necessarily represent the official views of the National Institutes of Health.*

Conflict of interest

The authors declare that they have no conflicts of interest with the contents of this article.

Abbreviations

AKI, acute kidney injury; *B2m*, beta-2-microglobulin; BUN, blood urea nitrogen; CC3, cleaved caspase 3; CHOP, C/EBP homologous protein; CKD, chronic kidney disease; CQ, chloroquine; *Cxcl1*, chemokine (C-X-C Motif) ligand 1; ERK, extracellular receptor kinase; *Il-6*, interleukin-6; IRE1 α , inositol requiring enzyme-1 alpha; JNK, c-jun n-terminal kinase; LC3B, microtubule associated protein light chain 3; *Mcp-1*, monocyte chemoattractant protein-1; nCDase, neutral ceramidase; NGAL, neutrophil gelatinase-associated lipocalin; p62, sequestosome 1/p62; PCNA, proliferating cell nuclear antigen; p-eIF2 α , phosphorylated- eukaryotic initiation factor 2 alpha; p-ERK, phosphorylated-extracellular receptor kinase; p-JNK, phosphorylated-c-jun n-terminal kinase; SIP, sphingosine-1-phosphate; SIPR1, SIP receptor 1; SCr, serum creatinine; *Tnfa*, tumor necrosis factor alpha.

Manuscript received January 18, 2022, and in revised form February 2, 2022. Published, JLR Papers in Press, February 10, 2022, <https://doi.org/10.1016/j.jlr.2022.100179>

REFERENCES

1. Dasari, S., and Tchounwou, P. B. (2014) Cisplatin in cancer therapy: molecular mechanisms of action. *Eur. J. Pharmacol.* **740**, 364–378
2. Makovec, T. (2019) Cisplatin and beyond: molecular mechanisms of action and drug resistance development in cancer chemotherapy. *Radiol. Oncol.* **53**, 148–158
3. Ghosh, S. (2019) Cisplatin: the first metal based anticancer drug. *Bioorg. Chem.* **88**, 102925
4. Miller, R. P., Tadagavadi, R. K., Ramesh, G., and Reeves, W. B. (2010) Mechanisms of cisplatin nephrotoxicity. *Toxins (Basel)*. **2**, 2490–2518
5. Ozkok, A., and Edelstein, C. L. (2014) Pathophysiology of cisplatin-induced acute kidney injury. *Biomed. Res. Int.* **2014**, 967826
6. Pabla, N., and Dong, Z. (2008) Cisplatin nephrotoxicity: mechanisms and renoprotective strategies. *Kidney Int.* **73**, 994–1007
7. Dupre, T. V., Sharp, C. N., and Siskind, L. J. (2018) 14.19 - Renal toxicology/nephrotoxicity of cisplatin and other chemotherapeutic agents. In *Comprehensive Toxicology*, 3rd Ed, C. A. McQueen, editor. Elsevier, Oxford, 452–486
8. Negi, S., Koreeda, D., Kobayashi, S., Yano, T., Tatsuta, K., Mima, T., Shigematsu, T., and Ohya, M. (2018) Acute kidney injury: epidemiology, outcomes, complications, and therapeutic strategies. *Semin. Dial.* **31**, 519–527
9. Basile, D. P., Anderson, M. D., and Sutton, T. A. (2012) Pathophysiology of acute kidney injury. *Compr. Physiol.* **2**, 1303–1353
10. Skinner, R., Parry, A., Price, L., Cole, M., Craft, A. W., and Pearson, A. D. (2009) Persistent nephrotoxicity during 10-year follow-up after cisplatin or carboplatin treatment in childhood: relevance of age and dose as risk factors. *Eur. J. Cancer.* **45**, 3213–3219
11. Sato, Y., Takahashi, M., and Yanagita, M. (2020) Pathophysiology of AKI to CKD progression. *Semin. Nephrol.* **40**, 206–215
12. Drexler, Y., Molina, J., Mitrofanova, A., Fornoni, A., and Merscher, S. (2021) Sphingosine-1-phosphate metabolism and signaling in kidney diseases. *J. Am. Soc. Nephrol.* **32**, 9–31
13. Dupre, T. V., and Siskind, L. J. (2018) The role of sphingolipids in acute kidney injury. *Adv. Biol. Regul.* **70**, 31–39
14. Abou Daher, A., El Jalkh, T., Eid, A. A., Fornoni, A., Marples, B., and Zeidan, Y. H. (2017) Translational aspects of sphingolipid metabolism in renal disorders. *Int. J. Mol. Sci.* **18**, 2528
15. Hannun, Y. A., and Obeid, L. M. (2008) Principles of bioactive lipid signalling: lessons from sphingolipids. *Nat. Rev. Mol. Cell Biol.* **9**, 139–150

16. Hannun, Y. A., and Obeid, L. M. (2018) Sphingolipids and their metabolism in physiology and disease. *Nat. Rev. Mol. Cell Biol.* **19**, 175–191
17. Mao, C., and Obeid, L. M. (2008) Ceramidases: regulators of cellular responses mediated by ceramide, sphingosine, and sphingosine-1-phosphate. *Biochim. Biophys. Acta.* **1781**, 424–434
18. Coant, N., Sakamoto, W., Mao, C., and Hannun, Y. A. (2017) Ceramidases, roles in sphingolipid metabolism and in health and disease. *Adv. Biol. Regul.* **63**, 122–131
19. Malinina, L., and Brown, R. E. (2015) Catalytic mechanism of eukaryotic neutral ceramidase. *Structure.* **23**, 1371–1372
20. Coant, N., and Hannun, Y. A. (2019) Neutral ceramidase: advances in mechanisms, cell regulation, and roles in cancer. *Adv. Biol. Regul.* **71**, 141–146
21. Dupre, T. V., Doll, M. A., Shah, P. P., Sharp, C. N., Siow, D., Megyesi, J., Shayman, J., Bielawska, A., Bielawski, J., Beverly, L. J., Hernandez-Corbacho, M., Clarke, C. J., Snider, A. J., Schnellmann, R. G., Obeid, L. M., *et al.* (2017) Inhibiting glucosylceramide synthase exacerbates cisplatin-induced acute kidney injury. *J. Lipid Res.* **58**, 1439–1452
22. Sundaram, K., Mather, A. R., Marimuthu, S., Shah, P. P., Snider, A. J., Obeid, L. M., Hannun, Y. A., Beverly, L. J., and Siskind, L. J. (2016) Loss of neutral ceramidase protects cells from nutrient- and energy-deprivation-induced cell death. *Biochem. J.* **473**, 743–755
23. Jiang, M., Wei, Q., Dong, G., Komatsu, M., Su, Y., and Dong, Z. (2012) Autophagy in proximal tubules protects against acute kidney injury. *Kidney Int.* **82**, 1271–1283
24. Takahashi, A., Kimura, T., Takabatake, Y., Namba, T., Kaimori, J., Kitamura, H., Matsui, I., Niimura, F., Matsusaka, T., Fujita, N., Yoshimori, T., Isaka, Y., and Rakugi, H. (2012) Autophagy guards against cisplatin-induced acute kidney injury. *Am. J. Pathol.* **180**, 517–525
25. Novgorodov, S. A., Riley, C. L., Yu, J., Borg, K. T., Hannun, Y. A., Proia, R. L., Kindy, M. S., and Gudiz, T. I. (2014) Essential roles of neutral ceramidase and sphingosine in mitochondrial dysfunction due to traumatic brain injury. *J. Biol. Chem.* **289**, 13142–13154
26. Kono, M., Dreier, J. L., Ellis, J. M., Allende, M. L., Kalkofen, D. N., Sanders, K. M., Bielawski, J., Bielawska, A., Hannun, Y. A., and Proia, R. L. (2006) Neutral ceramidase encoded by the *Ash2* gene is essential for the intestinal degradation of sphingolipids. *J. Biol. Chem.* **281**, 7324–7331
27. García-Barros, M., Coant, N., Kawamori, T., Wada, M., Snider, A. J., Truman, J.-P., Wu, B. X., Furuya, H., Clarke, C. J., Bialkowska, A. B., Ghaleb, A., Yang, V. W., Obeid, L. M., and Hannun, Y. A. (2016) Role of neutral ceramidase in colon cancer. *FASEB J.* **30**, 4159–4171
28. Zha, M., Tian, T., Xu, W., Liu, S., Jia, J., Wang, L., Yan, Q., Li, N., Yu, J., and Huang, L. (2020) The circadian clock gene *Bmal1* facilitates cisplatin-induced renal injury and hepatization. *Cell Death Dis.* **11**, 446
29. Cao, B. B., Li, D., Xing, X., Zhao, Y., Wu, K., Jiang, F., Yin, W., and Li, J. D. (2018) Effect of cisplatin on the clock genes expression in the liver, heart and kidney. *Biochem. Biophys. Res. Commun.* **501**, 593–597
30. Sears, S. M., Sharp, C. N., Krueger, A., Oropilla, G. B., Saforo, D., Doll, M. A., Megyesi, J., Beverly, L. J., and Siskind, L. J. (2020) C57BL/6 mice require a higher dose of cisplatin to induce renal fibrosis and CCL2 correlates with cisplatin-induced kidney injury. *Am. J. Physiol. Renal Physiol.* **319**, F674–F685
31. Korrapati, M. C., Shaner, B. E., and Schnellmann, R. G. (2012) Recovery from glycerol-induced acute kidney injury is accelerated by suramin. *J. Pharmacol. Exp. Ther.* **341**, 126–136
32. Stallons, L. J., Whitaker, R. M., and Schnellmann, R. G. (2014) Suppressed mitochondrial biogenesis in folic acid-induced acute kidney injury and early fibrosis. *Toxicol. Lett.* **224**, 326–332
33. Dobyas, D. C., Levi, J., Jacobs, C., Kosek, J., and Weiner, M. W. (1980) Mechanism of cis-platinum nephrotoxicity: II. Morphologic observations. *J. Pharmacol. Exp. Ther.* **213**, 551–556
34. Mandic, A., Hansson, J., Linder, S., and Shoshan, M. C. (2003) Cisplatin induces endoplasmic reticulum stress and nucleus-independent apoptotic signaling. *J. Biol. Chem.* **278**, 9100–9106
35. Mauthe, M., Orhon, I., Rocchi, C., Zhou, X., Luhr, M., Hijlkema, K. J., Coppes, R. P., Engedal, N., Mari, M., and Reggiori, F. (2018) Chloroquine inhibits autophagic flux by decreasing autophagosome-lysosome fusion. *Autophagy.* **14**, 1435–1455
36. Schrezenmeier, E., and Dörner, T. (2020) Mechanisms of action of hydroxychloroquine and chloroquine: implications for rheumatology. *Nat. Rev. Rheumatol.* **16**, 155–166
37. Zidovetzki, R., Sherman, I. W., Cardenas, M., and Borchardt, D. B. (1993) Chloroquine stabilization of phospholipid membranes against diacylglycerol-induced perturbation. *Biochem. Pharmacol.* **45**, 183–189
38. Siskind, L. J., Mullen, T. D., Romero Rosales, K., Clarke, C. J., Hernandez-Corbacho, M. J., Edinger, A. L., and Obeid, L. M. (2010) The BCL-2 protein BAK is required for long-chain ceramide generation during apoptosis. *J. Biol. Chem.* **285**, 11818–11826
39. Yabu, T., Shiba, H., Shibasaki, Y., Nakanishi, T., Imamura, S., Touhata, K., and Yamashita, M. (2015) Stress-induced ceramide generation and apoptosis via the phosphorylation and activation of nSMase1 by JNK signaling. *Cell Death Differ.* **22**, 258–273
40. Iwata, M., Herrington, J., and Zager, R. A. (1995) Sphingosine: a mediator of acute renal tubular injury and subsequent cytoresistance. *Proc. Natl. Acad. Sci. U. S. A.* **92**, 8970–8974
41. Snider, A. J., Wu, B. X., Jenkins, R. W., Sticca, J. A., Kawamori, T., Hannun, Y. A., and Obeid, L. M. (2012) Loss of neutral ceramidase increases inflammation in a mouse model of inflammatory bowel disease. *Prostaglandins Other Lipid Mediat.* **99**, 124–130
42. Bajwa, A., Rosin, D. L., Chroscicki, P., Lee, S., Dondeti, K., Ye, H., Kinsey, G. R., Stevens, B. K., Jobin, K., Kenwood, B. M., Hoehn, K. L., Lynch, K. R., and Okusa, M. D. (2015) Sphingosine 1-phosphate receptor-1 enhances mitochondrial function and reduces cisplatin-induced tubule injury. *J. Am. Soc. Nephrol.* **26**, 908–925
43. Okusa, M. D., and Lynch, K. R. (2007) Targeting sphingosine 1 phosphate receptor type 1 receptors in acute kidney injury. *Drug Discov. Today Dis. Mech.* **4**, 55–59
44. Awad, A. S., Ye, H., Huang, L., Li, L., Foss, F. W., Jr., Macdonald, T. L., Lynch, K. R., and Okusa, M. D. (2006) Selective sphingosine 1-phosphate 1 receptor activation reduces ischemia-reperfusion injury in mouse kidney. *Am. J. Physiol. Renal Physiol.* **290**, F1516–F1524
45. Perry, H. M., Huang, L., Ye, H., Liu, C., Sung, S. J., Lynch, K. R., Rosin, D. L., Bajwa, A., and Okusa, M. D. (2016) Endothelial sphingosine-1 phosphate receptor-1 mediates protection and recovery from acute kidney injury. *J. Am. Soc. Nephrol.* **27**, 3383–3393
46. Bajwa, A., Jo, S. K., Ye, H., Huang, L., Dondeti, K. R., Rosin, D. L., Haase, V. H., Macdonald, T. L., Lynch, K. R., and Okusa, M. D. (2010) Activation of sphingosine-1-phosphate 1 receptor in the proximal tubule protects against ischemia-reperfusion injury. *J. Am. Soc. Nephrol.* **21**, 955–965
47. Bajwa, A., Huang, L., Kurmaeva, E., Gigliotti, J. C., Ye, H., Miller, J., Rosin, D. L., Lobo, P. I., and Okusa, M. D. (2016) Sphingosine 1-phosphate receptor 3-deficient dendritic cells modulate splenic responses to ischemia-reperfusion injury. *J. Am. Soc. Nephrol.* **27**, 1076–1090
48. Bajwa, A., Huang, L., Ye, H., Dondeti, K., Song, S., Rosin, D. L., Lynch, K. R., Lobo, P. I., Li, L., and Okusa, M. D. (2012) Dendritic cell sphingosine 1-phosphate receptor-3 regulates Th1-Th2 polarity in kidney ischemia-reperfusion injury. *J. Immunol.* **189**, 2584–2596
49. Harvald, E. B., Olsen, A. S. B., and Færgeman, N. J. (2015) Autophagy in the light of sphingolipid metabolism. *Apoptosis.* **20**, 658–670
50. Guenther, G. G., Peralta, E. R., Rosales, K. R., Wong, S. Y., Siskind, L. J., and Edinger, A. L. (2008) Ceramide starves cells to death by downregulating nutrient transporter proteins. *Proc. Natl. Acad. Sci. U. S. A.* **105**, 17402–17407
51. Scarlatti, F., Bauvy, C., Ventruti, A., Sala, G., Cluzeaud, F., Vandewalle, A., Ghidoni, R., and Codogno, P. (2004) Ceramide-mediated macroautophagy involves inhibition of protein kinase B and up-regulation of beclin 1. *J. Biol. Chem.* **279**, 18384–18391
52. Lavieu, G., Scarlatti, F., Sala, G., Carpentier, S., Levade, T., Ghidoni, R., Botti, J., and Codogno, P. (2006) Regulation of autophagy by sphingosine kinase 1 and its role in cell survival during nutrient starvation. *J. Biol. Chem.* **281**, 8518–8527
53. Chang, C. L., Ho, M. C., Lee, P. H., Hsu, C. Y., Huang, W. P., and Lee, H. (2009) SIP(5) is required for sphingosine 1-phosphate-induced autophagy in human prostate cancer PC-3 cells. *Am. J. Physiol. Cell Physiol.* **297**, C451–C458
54. Sharp, C. N., Doll, M. A., Megyesi, J., Oropilla, G. B., Beverly, L. J., and Siskind, L. J. (2018) Subclinical kidney injury induced by repeated cisplatin administration results in progressive chronic kidney disease. *Am. J. Physiol. Renal Physiol.* **315**, F161–F172
55. Sears, S., and Siskind, L. (2021) Potential therapeutic targets for cisplatin-induced kidney injury: lessons from other models of AKI and fibrosis. *J. Am. Soc. Nephrol.* **32**, 1559–1567